Structural insights into biased G protein-coupled receptor signaling revealed by fluorescence spectroscopy.

Rita Rahmeh, Marjorie Damian, Martin Cottet, Hélène Orcel, Christiane Mendre, Thierry Durroux, K Shivaji Sharma, Grégory Durand, Bernard Pucci, Eric Trinquet, et al.

Title page

Structural insights into biased GPCR signaling revealed by fluorescence spectroscopy

Rita Rahmeh[1], Marjorie Damian[2], Martin Cottet[1], Hélène Orcel[1], Christiane Mendre[1], Thierry Durroux[1], K. Shivaji Sharma[2,3], Grégory Durand[2,3], Bernard Pucci[2,3], Eric Trinquet[4], Jurriaan M. Zwier[4], Xavier Deupi[5], Patrick Bron[6], Jean-Louis Banères[2], Bernard Mouillac[1]*, and Sébastien Granier[1]*

[1] CNRS UMR 5203, and INSERM U661, and Université Montpellier 1 et 2, Institut de Génomique Fonctionnelle, 141 rue de la Cardonille 34094 Montpellier cedex 05, France

[2] CNRS UMR 5247, and Université Montpellier 1 et 2, Institut des Biomolécules Max Mousseron, 15 avenue Charles Flahault 34093 Montpellier cedex 05, France

[3] Université d'Avignon et des Pays de Vaucluse, Equipe Chimie Bioorganique et Systèmes Amphiphiles, 33 rue Louis Pasteur, F-84000 Avignon, France

[4] Cisbio Bioassays, Parc technologique Marcel Boiteux, Bagnols/Cèze cedex F-30204, France

[5] Condensed Matter Theory Group and Laboratory of Biomolecular Research, Paul Scherrer Institut, 5232 Villigen PSI, Switzerland.

[6] CNRS UMR 5048, and INSERM U554, and Université Montpellier 1 et 2, Centre de Biochimie Structurale, 29 rue de Navacelles 34090 Montpellier cedex, France

*Correspondence should be addressed to S.G. (sebastien.granier@igf.cnrs.fr) or B.M.(bernard.mouillac@igf.cnrs.fr)

Abstract

G protein-coupled receptors (GPCRs) are seven-transmembrane proteins that mediate most cellular responses to hormones and neurotransmitters, representing the largest group of therapeutic targets. Recent studies show that some GPCRs signal through both G protein and arrestin pathways in a ligand-specific manner. Ligands that direct signaling through a specific pathway are known as biased ligands. The arginine-vasopressin type 2 receptor (V2R), a prototypical peptide-activated GPCR, is an ideal model system to investigate the structural basis of biased signaling. While the native hormone arginine-vasopressin leads to activation of both Gs (the stimulatory G protein for adenylyl cyclase) and arrestin pathways, synthetic ligands exhibit highly biased signaling through either Gs alone or arrestin alone. We used purified V2R stabilized in neutral amphipols and developed fluorescence-based assays to investigate the structural basis of biased signaling for the V2R. Our studies demonstrate that the Gs biased agonist stabilizes a conformation that is distinct from that stabilized by the arrestin biased agonists. This study provides new insights into the structural mechanisms of GPCR activation by biased ligands that may be relevant to the design of pathway-biased drugs.

\body

Introduction

G protein-coupled receptors (GPCRs) constitute the largest family of membrane proteins. They are responsible for the majority of cellular responses to a broad range of stimuli, including peptide and non-peptide neurotransmitters, hormones, growth factors, odorant molecules and light. GPCRs play critical roles in regulating most physiological functions and, thus, are the targets of 30% of currently marketed drugs(1).

To understand the function of GPCRs at the molecular level, it is fundamental to investigate the nature of the structural rearrangements that couple ligand binding to receptor-dependent activation of downstream signaling pathways. It is now clear that a given ligand is able to induce multiple signaling pathways such as activation of G proteins and β-arrestin mediated pathways(2). Accordingly, the traditional ligand classification into agonists, partial agonists, antagonists and inverse agonists cannot be restricted to activation of a single signaling pathway. For instance, a given ligand can act as an inverse agonist of the Gs pathway and as an agonist of β-arrestin signaling cascade(3). These ligand properties have a potential clinical relevance as suggested by a recent study on the beta-blocker carvedilol(4). Initially termed 'agonist-selective trafficking of receptor signaling(5), this concept is now also described as the 'functional selectivity or biased agonism' of a GPCR ligand(6).

It is known from several biophysical studies on purified β2-adrenergic receptor (β2AR), as well as on α_{2a}-adrenergic receptor in living cells, that binding of different classes of ligands induce distinct conformational changes in these receptors(7, 8), suggesting a high degree of structural plasticity in GPCRs(9). GPCR conformational

changes associated to ligand binding are responsible for G-protein coupling and β-arrestin recruitment(10, 11).

Cell-based studies suggest that functional selectivity arises as a result of distinct conformational states of the receptor stabilized by the ligands(12, 13). In this context, establishing links between functional selectivity and distinct conformational states of GPCRs is of primary importance. However, only limited information is available concerning receptor molecular switches involved in ligand-dependent efficacy and functional selectivity. Moreover, the molecular mechanisms underlying the functional selectivity property of so-called biased agonist ligands remain elusive.

To study the molecular mechanisms responsible for ligand efficacy and functional selectivity, we directly monitored conformational changes induced by either biased or unbiased ligands within a prototypic peptide-activated GPCR, the V2 arginine-vasopressin (AVP) receptor (V2R) using two fluorescence-based approaches: tryptophan intrinsic fluorescence spectroscopy and lanthanide resonance energy transfer (LRET)(14). For LRET measurements, two fluorophores were introduced into domains important for G protein coupling and for interaction with β-arrestin(15, 16). The donor was fused either to the cytoplasmic end of the transmembrane domain 6 (TM6) or to the cytoplasmic end of the transmembrane domain 7 (TM7) just before the putative helix 8 sequence. The acceptor was attached at the extreme C-terminus domain of the receptor. V2R represents an interesting model to study molecular bases of functional selectivity for several reasons; i) its pharmacology has been well-characterized using a large panel of ligands with different efficacies toward the Gs signaling pathway(17) and ii) several V2R ligands are biased agonists. For instance, while the unbiased natural hormone AVP is a full agonist towards Gs protein and β-arrestin (Gs agonist / Arr agonist), two non-peptide biased synthetic

ligands, MCF14 (Gs agonist / Arr antagonist) and SR121463 (Gs inverse agonist / Arr partial agonist) have been described(12, 18).

In this study, we first demonstrate that purified V2R functionally reconstituted into a neutral amphipol (NAPol(s))(19) responds to ligands with the same efficacy profiles towards activation of purified Gs protein and arrestin-2 (β-arrestin-1) as in living cells. We then analyzed the effects of biased ligands on the receptor structure. We found that changes in the tryptophan intrinsic fluorescence upon ligand binding correlated well with the efficacy profile of ligands towards the G protein signaling pathway. LRET spectroscopy measurements showed that ligands exhibiting different efficacies (full agonist, antagonist or inverse agonist) towards G protein activation and arrestin recruitment stabilize distinct conformations of the V2R. Taken together, our study demonstrates that ligand-dependent arrestin recruitment by GPCRs is triggered by specific conformational movements that are different from the conformational changes responsible for G protein activation.

RESULTS

Reconstitution of purified V2R in amphipol

The Flag-tagged V2R (Flag-V2R) was expressed in insect cells by using recombinant baculovirus technology. Flag-V2R is properly expressed at the plasma membrane of Sf9 cells, binds [^{3}H]-AVP with an affinity similar to receptor expressed in mammalian cells (Kd = 13.5 ± 0.7 nM) (**Supporting Fig. S1a and S1b**) and is able to couple to Gs protein (**Supporting Fig. S1c**). The Flag-V2R was purified by immuno-chromatography using a M1 Flag antibody affinity resin (**Fig. 1a)** and reconstituted by exchanging detergents for neutral amphipols (NAPol(s), 1:10 protein:NAPol(s) weight ratio) which are known to enhance the stability of membrane

5

proteins (20). In order to obtain a homogeneous fraction of the V2R, the NAPol(s)-reconstituted receptors were then loaded onto a size exclusion chromatography column. A receptor population was eluted at 15.5 ml close to the 75 kDa protein standards (Conalbumin) (**Fig. 1b**). Non-denaturing blue native-PAGE analysis (**Fig. 1b)** revealed NAPol(s) reconstituted V2R at around 75-80 kDa. These results are consistent with the molecular weight of a monomeric V2R (42 kDa) that would be in complex with at least 3 molecules of NAPol(s) on average(19). The enriched monomeric fraction was then used throughout the study. The particles containing the V2R were then visually inspected by negative staining electron microscopy. Images analyses from electron micrograph of the monomeric V2R-containing sample are shown in **Fig. 1c**. It reveals the presence of apparently homogeneous population of particles having a round shape with a diameter ranging from 7 to 10 nm. Finally, we analyzed the pharmacological properties of V2R reconstituted in NAPol(s) using [^{3}H]-AVP saturating experiments (**Fig. 1d).** We determined an affinity constant of 674 ± 90 nM. Using the calculated Bmax value we evaluated the active fraction of receptor at about 90% of the total protein amount **(see supporting information)**.

Effect of ligands on G protein activation and recruitment of arrestin-2 by NAPol(s)-reconstituted V2R.

To determine the functionality of NAPol(s)-reconstituted V2R, we first measured ligand-induced incorporation of [^{35}S]GTPγS to purified Gαs proteins (1:2.5 receptor:G protein molar ratio). This assay was done using two full agonists for the Gs pathway, the endogenous hormone AVP and the biased ligand MCF14(18)**,** and also with a Gs inverse agonist (SR121463)(21) (**Fig. 2a**). The effects of ligands (10 µM) were compared to a basal signaling (i.e. basal [35S]-GTPγS binding to the subunit Gαs). As shown in **Fig. 2b**, V2R induced a 1.42 -fold increase in

[35S]GTPγS incorporation over basal, suggesting a constitutive activity towards Gαs. The full agonists elicited similar GTPγS incorporation (3.22 and 2.95 -fold over basal) whereas the inverse agonist treatment reduced the constitutive activity of the untreated V2R-Gαs complex by 50% (**Fig. 2b)**. These results demonstrate that NAPol-reconstituted V2R interacts with and efficiently activates Gs protein in a ligand-dependent manner. Importantly, the efficacy profiles of the ligands correlated well with those observed in living cells(18, 21)**.**

It has been shown that AVP activation of the V2R induces a stable interaction with both arrestin-2 and 3(22)**.** In addition, SR121463 which is a V2R inverse agonist for the Gs protein pathway has been described as a partial agonist for the arrestin pathway(12) defining this compound as an arrestin biased ligand. To determine the ability of ligands to modulate the recruitment of arrestin-2 by the NAPol(s)-reconstituted V2R, we measured direct interactions between the receptor and a monobromobimane-labeled purified arrestin-2 (1:1 arrestin:receptor molar ratio, 10 μM). Bimane is a small size fluorophore with a high sensitivity to the polarity of its molecular environment that can be used as a sensor to detect interactions between the arrestin and its protein partners, as observed for visual arrestin and rhodopsin(23)**.** As illustrated in **Fig. 2c**, incubation of arrestin-2 with NAPol(s)-reconstituted V2R led to a quenching of 54 $\pm$ 5 % of the bimane fluorescence intensity, suggesting a high constitutive interaction of the two proteins. Typical fluorescence spectra of the bimane-labeled arrestin are provided in the **supporting figure S2** in the absence or presence of V2R and after AVP treatment. In the presence of the full agonist AVP and the partial agonist (SR121463), we observed a fluorescence quenching of 77 $\pm$ 3 % and 65 $\pm$ 4 %, respectively. On the contrary, the Gs-biased MCF14, an agonist for the Gs pathway and an antagonist for the V2R-

arrestin pathway(18), did not induce a change in fluorescence intensity **(Fig. 2c)**. Moreover, we found that the AVP-induced fluorescence quenching can be reversed by MCF14 as expected for an antagonist. To rule out the possibility that the NAPol(s) by itself had an effect on the quenching of the fluorophore, the receptor-free amphipol was incubated with bimane-labeled purified arrestin-2 and with or without AVP. No change in the fluorescence of bimane was recorded in these conditions (**Fig. 2c**).

These results demonstrate that the monomeric NAPol(s)-reconstituted V2R efficiently interacts with arrestin-2 and that the efficacy profiles of the ligands correlate with those observed in living cells.

Effect of ligands on the intrinsic tryptophan fluorescence of the V2R.

The fluorescent properties of tryptophans are very sensitive to their local chemical environment. There are 11 tryptophans distributed primarily in the TM segments (TM) including in TMs 2, 4, 5, 6 and 7. Therefore, tryptophan fluorescence can provide information about ligand-specific changes in the transmembrane core of the V2R. As shown in **Fig. 3a**, addition of SR121463, (Gs inverse agonist / Arr partial agonist), induced a 21 ± 1.7 % decrease of the intrinsic tryptophan fluorescence intensity. On the other hand, AVP (Gs agonist / Arr agonist) led to an increase of 8 ± 0.9 % (**Fig. 3b**). Similarly, MCF14 (Gs agonist /Arr antagonist), induced an increase of 10 ± 2 % (**Fig. 3b**). As a control, we did not observe any changes in tryptophan intrinsic fluorescence when we added SR121463, AVP and MCF14 to the unfolded receptor (0.61 ± 1 %, 0.6 ± 2 %, 1 ± 0.6 %, respectively compared to the untreated receptor). We also determined the ligand concentration dependence on the tryptophan fluorescence signals and determined EC50s for AVP (1.13 ± 0.5 µM),

MCF14 (2.28 ± 0.8 µM) and SR121463 (2.86 ± 0.7 µM) as described in **supporting information** and in the **supporting Figure S3.**

Our results thus show that ligands with different efficacies towards Gs and arrestin signaling pathways induce opposite changes in intrinsic tryptophan fluorescence suggesting that these ligands induce distinct conformational changes within the receptor that are necessary for pathway-selective signaling. However, intrinsic tryptophan fluorescence only gives information about global conformational changes in the receptor, but cannot report on molecular movements from specific structural domains.

LRET reveals two basal V2R states

Fluorescence resonance energy transfer (FRET) has been used to study conformational changes in the β_2AR (24)**.** This approach requires site-specific labeling of the protein with two different fluorescent probes. We developed a related approach based on resonance energy transfer (RET), known as lanthanide-based or luminescence RET (LRET, see **supporting information**). We used two mutants for the LRET experiments (depicted schematically in **Fig. 4**) for which the site-specific labeling and the biochemistry were carefully characterized (**supporting information, supporting Fig. S4 and S5**). For clarity, the Flag-V2R-A267C-C358A-FlAsH mutant will be noted TM6 sensor and the Flag-V2R-S330C-C358A-FlAsH, TM7-H8 sensor. Based on ligand binding and Gs-dependent cAMP accumulation in insect cells, the function of both mutants appeared equivalent to that of the wild-type receptor (**Supporting Fig. S1c**).

LRET measurements were performed as described in the Material and Methods section. Our results show that the fluorescence decay of the donor-only species is

adequately fit by a one component exponential function for both sensors **(Fig. 4a and 4b)**. In contrast, the fluorescence decay of the donor in the presence of acceptor is best fit with a two component exponential function **(Fig. 4a and 4b)** suggesting the presence of two distinct lifetimes. This measurement is made by monitoring the decay of the sensitized acceptor emission so that only the donor and acceptor engaged in LRET is detected (**supporting information**), We observed no intermolecular LRET in samples containing receptor labeled only with donor mixed with equivalent amounts of receptor labeled only with acceptor (**Supporting Fig. S6**).

These LRET data suggests the existence of at least two distinct basal states of the V2R characterized by distinct lifetimes constants of acceptor-sensitized emission (τ_{AD} fast and τ_{AD} slow, fast population and slow population) in both the TM6 and TM7-H8 sensor.

Effect of ligands on the conformational states of V2R revealed by LRET

To study ligand-dependent conformational changes in the V2R, we monitored the effects of AVP (Gs agonist / Arr agonist), SR121463 (Gs inverse agonist / Arr partial agonist) and MCF14 (Gs agonist / Arr antagonist) on the LRET signals for the TM6 sensor and TM7-helix 8 sensor. **Fig. 5a and 5b** show typical acceptor-sensitized fluorescence decays on a linear scale obtained with untreated TM6 sensor and TM7-H8 sensor, respectively (black trace) and after treatment with the full agonist AVP (red trace). The lifetime analysis revealed in this case significant changes in τ_{AD} fast and τ_{AD} slow after AVP treatment **(Fig. 5c and 5d)**.

We then analyzed the effect of biased ligands on the LRET signals. For clarity and as discussed in the **supporting information**, only the effect on the largest

population is shown in **Fig. 6** (slow population). Importantly, the effects on both receptor populations follow a similar trend for both sensors (**Supporting Table S1**).

The results show a clear correlation between the ligands efficacy and their effect on lifetimes values (**Fig. 6,** top panel representing the ligands efficacy, and bottom panel their effects on lifetime measurements). First, for the TM6 sensor, AVP and MCF14 (full agonists towards G protein, **Fig. 6a top panel**) induced an increase in the lifetime $\vert_{AD}$ (26 ± 1 % and 23 ± 3 %, respectively, **Fig. 6a bottom panel**), whereas treatment of the receptor with the Gs inverse agonist SR121463 (**Fig. 6a top panel**) led to an opposite effect with a decreased lifetime (**Fig. 6a, bottom panel**).

For the TM7-H8 sensor, AVP (Arr full agonist) and SR121463 (Arr partial agonist) (**Fig. 6b top panel**) induced an increase of 27 ± 7 % and 31 ± 6 % of $\vert_{AD}$, respectively (**Fig. 6b, bottom panel**). Finally, treatment of the receptor with the Arr antagonist, MCF14 (**Fig. 6b top panel)**, did not induce a significant change in lifetime measurements (**Fig. 6b, bottom panel**). As a control, under the same conditions we did not observe any changes in the lifetimes $\vert_{AD}$ when we treated the receptor with Leuprolide, an unrelated nonapeptide acting as an agonist for the GnRH receptor(25) **(Supporting Table S1)**.

To address the contribution of the background labeling on the LRET results, we measured the amount of Lumi4-Tb incorporated into the Flag-V2R-C358A-FlAsH receptor. The ratio of Lumi4-Tb labeling is 0.2 instead of 0.5 to 0.7 for TM6 and TM7-H8 sensors (**supporting information**). This level labeling level did not allow us to measure any LRET when using a receptor concentration equivalent to that used for TM6 or TM7-H8 sensors (0.1 µM). By increasing the amount of protein used in the

LRET experiment (0.5 µM) we were able to detect significant LRET. In this condition, as for the two other sensors, we measured two lifetime components (**Supporting Table 1 and Supporting Fig. S8a**). However, we cannot directly compare this background labeling to that of the TM6 and TM7/H8 sensors because in the absence of the most reactive cysteine, the probes will necessarily react with the low reactive cysteines thus increasing the amount of background. In the presence of the reactive cysteine, one would expect a ratio of background labeling much lower than 0.2. It is unlikely that this level of background labeling influences our results since both SR and MCF induce opposite effects on receptor labeled specifically at the TM6 or TM7-H8 sensors.

DISCUSSION

GPCRs are known to activate different signaling pathways that can be differentially regulated by specific ligands. This phenomenon is described as functional selectivity or biased agonism. However, the mechanisms by which biased ligands can control the signaling outcome of a receptor at the molecular level are not yet known. Here, we used the AVP V2R subtype as a GPCR model to address this question. We used tryptophan and LRET spectroscopy, to investigate ligand-specific conformational changes in purified V2R reconstituted into neutral amphipols.

Purified V2R reconstituted in neutral amphipols is functional and couples to both Gs protein and arrestin-2 with the same efficacy profiles as observed in living cells. Using this system, we show that the signaling properties of the receptor are achieved through the stabilization of distinct conformational states by ligands. Our data suggest that movements of TM6-i3 are required for G protein activation/inhibition but may not be involved in the selective recruitment of arrestin. On the other hand,

movements between the TM7-helix8 are required for selective recruitment of arrestin. These results provide evidence for a direct conformational link between the ligand binding pocket and the intracellular surface of the receptor, supporting a model whereby binding of structurally different ligands to a common orthosteric site induce or stabilize specific set confomational states that dictate the interactions between the V2R and cytoplasmic signaling molecules.

Consistent with the dynamic nature of GPCR(11), our LRET data provide evidence for two distinct conformations of V2R in the basal state. Indeed, these two populations are also detected in presence of ligands, and their relative distribution is not significantly affected (**Supporting Table S1**). It is thus unlikely that they represent equilibrium between an active and inactive form of the receptor.

Using the time constants of acceptor-sensitized emission (τ_{AD} fast and τ_{AD} slow) and donor-only emission (τ_D), we calculated the distances between donor and acceptor both for the TM6 sensor and in the TM7-H8 sensor (Materials and Methods section and **Supporting Table S1**). According to these calculations, the estimated difference in the two distances (fast and slow) between the TM6 and the C-terminus, or between the TM7-H8 and the C-terminus is around 10 Å. We thus suggest that the position of the C-terminus is the main structural difference between the two conformations present in the basal state, possibly due to some heterogeneity in phosphorylation or palmitoylation; however, we cannot exclude structural heterogeneity in TM6 and in TM7-H8.

The changes in LRET in the presence of different ligands can be attributed to changes in distance between the donor and acceptor probes (**Supporting Table S1**). While these calculated changes are small (the largest being 2.5Å increase in

the distance between cytoplasmic end of TM6 and the extreme C-terminus of the V2R), it is known that molecular movements as little as 1 Å can lead to profound modifications on the activity of enzymes and receptors(26). Accordingly, these minor movements may also have important effects in the GPCR-G protein and arrestin coupling/uncoupling mechanisms. In agreement with our data, the recent crystal structures of a nanobody-stabilized β2-AR active state and of the β2-AR-Gs protein complex revealed a large movement of the TM6 in comparison with the inverse agonist-bound structures(27, 28). Although less dramatically the TM7-H8 region is also moving during activation(29). These movements were also detected using DEER spectroscopy in rhodopsin (30).

To reconcile our data obtained with the TM6 and the TM7-H8 sensors, we propose that the functional outcome of ligand binding depends on the effect that they trigger in the TM6-icl3 (Gs activity) and in the TM7-H8 (arrestin activity) domains, which can be considered molecular switches for the activation of intracellular partners (**Fig. 7**). While the full agonist AVP affects both molecular switches and, thus, is able to activate both signalling pathways, MCF is only able to trigger the TM6 switch and activate Gs. On the other hand, SR is able to reduce the activity of the G protein and promote arrestin recruitment by constraining the TM6 molecular switch and activating the TM7-H8 domain.

Importantly, our data demonstrate that ligand-dependent arrestin recruitment by the receptor is triggered by conformational states that are distinct from those responsible for Gs protein activation, laying the foundation for a structural mechanism of ligand-induced biased signalling.

MATERIALS AND METHODS

Preparation of V2R/NAPol(s) complexes

Construction, expression, solubilization and purification of the receptor mutants from Sf9 insect cells as well as the labeling kinetics methods are described in the **supporting information**. Purified detergent-soluble receptors were incubated at 4°C in the presence of the amphipols at a 1:10 protein:NAPol(s) weight ratio(19). After detergent removal with Bio-beads, the sample was subjected to size exclusion chromatography (see **supporting information)** to isolate the monomeric fraction of V2R. The V2R/NAPol(s) complexes were then characterized by negative-stain transmission EM as described in the **supporting information.**

[^{35}S]-GTPγS binding and Arrestin-2 recruitement assays

Gαs protein was produced and purified as described in the **supporting information**. Binding experiments were performed as described in the **supporting information.** The arrestin-2 mutant L68C-R169E was produced in E.coli and purified by IMAC as described in the **supporting information.** The purified protein was then labelled with monobromobimane as described in Sommer et al.(23) and the arrestin recruitement assays were performed as described in the **supporting information.**

Analysis of LRET Data

Luminescence emission decays were measured at 620 nm and 520 nm and fitted as described in the **supporting information**. For acceptor-donor we calculated two lifetimes, defined as τ_{AD} fast and τ_{AD} slow. Ligand-induced changes in LRET and distances were measured as described in the **supporting information.** The

proportion of slow and fast populations was calculated as previously described(31) and details on the analysis are available in the **supporting information**.

ACKNOWLEDGMENTS

FOOTNOTES

S.G, B.M., J-L.B. and T.D. designed research. P.B performed the EM experiments. R.R., M.D., M.C., C.M., H.O., S.G. performed research and analyzed data. K.S.S., G.D., and B.P. contribute neutral amphipol reagents. E.T, J.Z contribute lanthanide reagents and help with the lifetimes analyses. X.D. built the receptor models to design the cysteine mutants for receptor labeling and helped with the interpretation of the LRET data. S.G., B.M and R.R. wrote the paper. S.G. originated the project and supervised the research with the help of B.M.

REFERENCES

1. Ma P & Zemmel R (2002) Value of novelty? *Nat Rev Drug Discov* 1(8):571-572
2. Rajagopal S, Rajagopal K, & Lefkowitz RJ (2010) Teaching old receptors new tricks: biasing seven-transmembrane receptors. *Nat Rev Drug Discov* 9(5):373-386
3. Kenakin T (2003) Ligand-selective receptor conformations revisited: the promise and the problem. *Trends Pharmacol Sci* 24(7):346-354
4. Wisler JW*, et al.* (2007) A unique mechanism of beta-blocker action: carvedilol stimulates beta-arrestin signaling. *Proc Natl Acad Sci U S A* 104(42):16657-16662
5. Kenakin T (1995) Agonist-receptor efficacy. II. Agonist trafficking of receptor signals. *Trends Pharmacol Sci* 16(7):232-238
6. Urban JD*, et al.* (2007) Functional selectivity and classical concepts of quantitative pharmacology. *J Pharmacol Exp Ther* 320(1):1-13
7. Swaminath G*, et al.* (2004) Sequential binding of agonists to the beta2 adrenoceptor. Kinetic evidence for intermediate conformational states. *J Biol Chem* 279(1):686-691
8. Zurn A*, et al.* (2009) Fluorescence resonance energy transfer analysis of alpha 2a-adrenergic receptor activation reveals distinct agonist-specific conformational changes. *Mol Pharmacol* 75(3):534-541
9. Kobilka BK (2007) G protein coupled receptor structure and activation. *Biochim Biophys Acta* 1768(4):794-807

10. Hoffmann C, Zurn A, Bunemann M, & Lohse MJ (2008) Conformational changes in G-protein-coupled receptors-the quest for functionally selective conformations is open. *Br J Pharmacol* 153 Suppl 1:S358-366

11. Kobilka BK & Deupi X (2007) Conformational complexity of G-protein-coupled receptors. *Trends Pharmacol Sci* 28(8):397-406

12. Azzi M*, et al.* (2003) Beta-arrestin-mediated activation of MAPK by inverse agonists reveals distinct active conformations for G protein-coupled receptors. *Proc Natl Acad Sci U S A* 100(20):11406-11411

13. Kenakin T (2007) Functional selectivity through protean and biased agonism: who steers the ship? *Mol Pharmacol* 72(6):1393-1401

14. Cha A, Snyder GE, Selvin PR, & Bezanilla F (1999) Atomic scale movement of the voltage-sensing region in a potassium channel measured via spectroscopy. *Nature* 402(6763):809-813

15. Erlenbach I & Wess J (1998) Molecular basis of V2 vasopressin receptor/Gs coupling selectivity. *J Biol Chem* 273(41):26549-26558

16. Benovic JL, Strasser RH, Caron MG, & Lefkowitz RJ (1986) Beta-adrenergic receptor kinase: identification of a novel protein kinase that phosphorylates the agonist-occupied form of the receptor. *Proc Natl Acad Sci U S A* 83(9):2797-2801

17. Manning M*, et al.* (2008) Peptide and non-peptide agonists and antagonists for the vasopressin and oxytocin V1a, V1b, V2 and OT receptors: research tools and potential therapeutic agents. *Prog Brain Res* 170:473-512

18. Jean-Alphonse F*, et al.* (2009) Biased agonist pharmacochaperones of the AVP V2 receptor may treat congenital nephrogenic diabetes insipidus. *J Am Soc Nephrol* 20(10):2190-2203

19. Bazzacco P*, et al.* (2009) Trapping and stabilization of integral membrane proteins by hydrophobically grafted glucose-based telomers. *Biomacromolecules* 10(12):3317-3326

20. Popot JL (2010) Amphipols, nanodiscs, and fluorinated surfactants: three nonconventional approaches to studying membrane proteins in aqueous solutions. *Annu Rev Biochem* 79:737-775

21. Morin D*, et al.* (1998) The D136A mutation of the V2 vasopressin receptor induces a constitutive activity which permits discrimination between antagonists with partial agonist and inverse agonist activities. *FEBS Lett* 441(3):470-475

22. Oakley RH, Laporte SA, Holt JA, Barak LS, & Caron MG (1999) Association of beta-arrestin with G protein-coupled receptors during clathrin-mediated endocytosis dictates the profile of receptor resensitization. *J Biol Chem* 274(45):32248-32257

23. Sommer ME, Smith WC, & Farrens DL (2005) Dynamics of arrestin-rhodopsin interactions: arrestin and retinal release are directly linked events. *J Biol Chem* 280(8):6861-6871

24. Granier S*, et al.* (2007) Structure and conformational changes in the C-terminal domain of the beta2-adrenoceptor: insights from fluorescence resonance energy transfer studies. *J Biol Chem* 282(18):13895-13905

25. Salvador A, Garcia-Paramio MP, Sanchez-Chapado M, Carmena MJ, & Prieto JC (2001) Effects of the luteinising hormone-releasing hormone (LH-RH) agonist leuprolide on adenylyl cyclase regulation through G-protein coupled receptors in rat ventral prostate. *Eur J Cancer* 37(5):641-648

26. Koshland DE, Jr. (1998) Conformational changes: how small is big enough? *Nat Med* 4(10):1112-1114

27. Rasmussen SG*, et al.* (2011) Structure of a nanobody-stabilized active state of the beta(2) adrenoceptor. *Nature* 469(7329):175-180

28. Rasmussen SG*, et al.* (2011) Crystal structure of the beta2 adrenergic receptor-Gs protein complex. *Nature* 477(7366):549-555

29. Choe HW*, et al.* (2011) Crystal structure of metarhodopsin II. *Nature* 471(7340):651-655

30. Altenbach C, Kusnetzow AK, Ernst OP, Hofmann KP, & Hubbell WL (2008) High-resolution distance mapping in rhodopsin reveals the pattern of helix movement due to activation. *Proc Natl Acad Sci U S A* 105(21):7439-7444

31. Posson DJ, Ge P, Miller C, Bezanilla F, & Selvin PR (2005) Small vertical movement of a K+ channel voltage sensor measured with luminescence energy transfer. *Nature* 436(7052):848-851

FIGURE LEGENDS

Figure 1. Purification of Flag-V2R, biochemical and pharmacological characterization of NAPol(s)-reconstituted V2R.

(**a**) Western blot analysis of Flag-V2R purified from Sf9 insect cells with an anti-Flag antibody. Molecular weight markers (Lane 1), solubilized membrane proteins (Lane 2), protein eluted from M1-Flag resin (Lane 3).

(**b**) Size-exclusion chromatography profile of NAPol(s)-reconstituted V2R and blue native-gel electrophoresis of the peak eluted at 15.5 ml corresponding to monomeric V2R reconstituted in NAPol(s).

(**c**) Analyses of electron micrograph of monomeric NAPol(s)-reconstituted V2R particles. Class averages obtained after images alignment cycles revealed three particles populations. Each image represents top and side views of the particles with their diameter.

(**d**) [^{3}H]-AVP saturating experiments on monomeric V2R reconstituted in NAPol(s). A representative binding curve (from a total of 3) is shown (each point corresponds to the mean value of triplicates).

Figure 2. Chemical structure and effect of ligands on G protein coupling and Arrestin-2 recruitment.

(**a**) Chemical structure of AVP (Gs agonist / Arr agonist), MCF14 (Gs agonist / Arr antagonist) and SR121463 (Gs inverse agonist/ Arr partial agonist).

(**b**) [^{35}S]-GTPγS binding to Gαs protein induced by ligand binding to NAPol(s)-reconstituted V2R. Gαs activity was measured as described under "Methods". [^{35}S]-GTPγS-specific binding induced by 10 µM AVP, MCF14 or SR121463 is represented as dpm. Data represent the mean ± s.e.m. of at least three independent experiments performed in triplicate.

(**c**) Arrestin-2 recruitement by NAPol(s)-reconstituted V2R. Specific recruitment of bimane-labeled arrestin-2 at position 68 (L68C) by V2R with or without 10 µM AVP, MCF14, SR121463 or both MCF14 and AVP is represented as a percentage of the fluorescence of bimane-labeled arrestin-2 in the presence of NAPol(s). Data represent the mean ± s.e.m. of three independent experiments performed in triplicate.

Figure 3. Effect of ligands on V2R tryptophan intrinsic fluorescence.

NAPol(s)-reconstituted V2R was incubated 15 minutes with or without the drug to be tested (AVP, MCF14 or SR121463, 10 µM). As a negative control, fluorescence of SDS-denatured V2R was measured in presence of SR121463, AVP and MCF14. (**a**) Typical spectra obtained for sample treated or not with SR121463 obtained as described in the **supporting information**. (**b**) An average of the intensity of tryptophan emission between 340 and 350 nm was calculated and normalized to that of untreated V2R ($I_{\lambda max(ligand)}/ I_{\lambda max(vehicle)}$). Data represent the mean ± s.e.m. of three independent experiments performed in triplicate. Statistical significance of differences from basal (V2R+vehicle) was assessed using Mann-Whitney test; **, $p < 0.01$, ***, $p < 0.001$.

Figure 4. V2R constructs used in LRET experiments and basal state V2R LRET measurement.

Schematic representation of Flag-V2R-A267C-C358A-FlAsH (TM6 sensor, **a**) and Flag-V2R-S330C-C358A-FlAsH (TM7-H8 sensor, **b**) constructs showing the position of the donor fluorophore (FlAsH, green) and the acceptor fluorophore (Lumi4-Tb, red). The Flag tag is shown in orange. Represented are the real size components as well as the linker for the Lumi4-Tb.

Luminescence emission decays from NAPol(s) reconstituted TM6 sensor (**a**) and TM7-H8 sensor (**b**) (0.1 µM) were measured as described in the Materials and Methods section. The terbium donor-only emission (black dots) and Flash-sensitized emission (grey dots) were fitted to exponential decay functions. The residual values represent the goodness of the fits. Each trace is the fluorescence decay measurement of a single well. Each measurement was analyzed independently and the lifetime was calculated as the average of three independent measurements for each experiment.

Figure 5. Changes in lifetimes upon AVP binding

Ligand-dependent sensitized emission changes of the TM6 sensor (**a**) and of the TM7-H8 sensor (**b**). Flash-sensitized emission in presence of vehicle (black trace), and AVP (red trace) are represented using a linear scale.

Calculated lifetimes (τAD fast and slow) before and after treatment with AVP for the TM6 sensor (**c**) and for the TM7-H8 sensor (**d**). Data represent the mean ± s.e.m. of six independent experiments. Values in percent represent the relative contribution of each of the components, slow and fast.

Figure 6. Correlation between ligand efficacy and their effects on lifetime measurements.
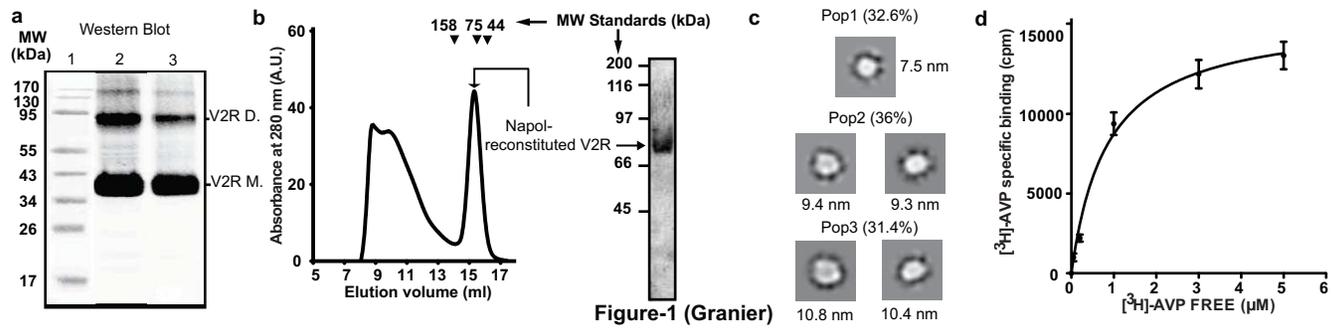
Efficacy of the ligands being used in this study for Gs (**a, top panel**) and for arrestin (**b, top panel**). A value of 1 for activity means full agonism. Negative activity represents inverse agonism and no activity means antagonism.

Percent changes in lifetimes (calculated as described in Methods) for the TM6 sensor (**a, bottom panel**) and for the TM7-H8 sensor (**b, bottom panel**).

Mann-Whitney test, **, $p < 0.01$

Figure 7. Model for ligand efficacy and functional selectivity.

AVP (Gs agonist / Arr agonist) induces fluorescence lifetime changes in both TM6 (grey arrow) and TM7-H8 (cyan arrows) sensors. MCF14 (Gs agonist / Arr antagonist) only induces changes in the TM6 sensor (grey arrow). SR121463 (Gs inverse agonist/ Arr partial agonist) modifies lifetimes for both the TM6 (black arrow, opposite changes than for AVP and MCF) and TM7-H8 sensors (similar changes than for AVP). These results suggest that the functional outcome of ligand binding depends on the effect that they trigger in the TM6-icl3 (Gs activity) and in the TM7-H8 (arrestin activity) domains. Numbers represent the % changes in fluorescence lifetime measurements (± s.e.m. for the slow population) upon ligand binding on TM6 and TM7-H8 sensors.
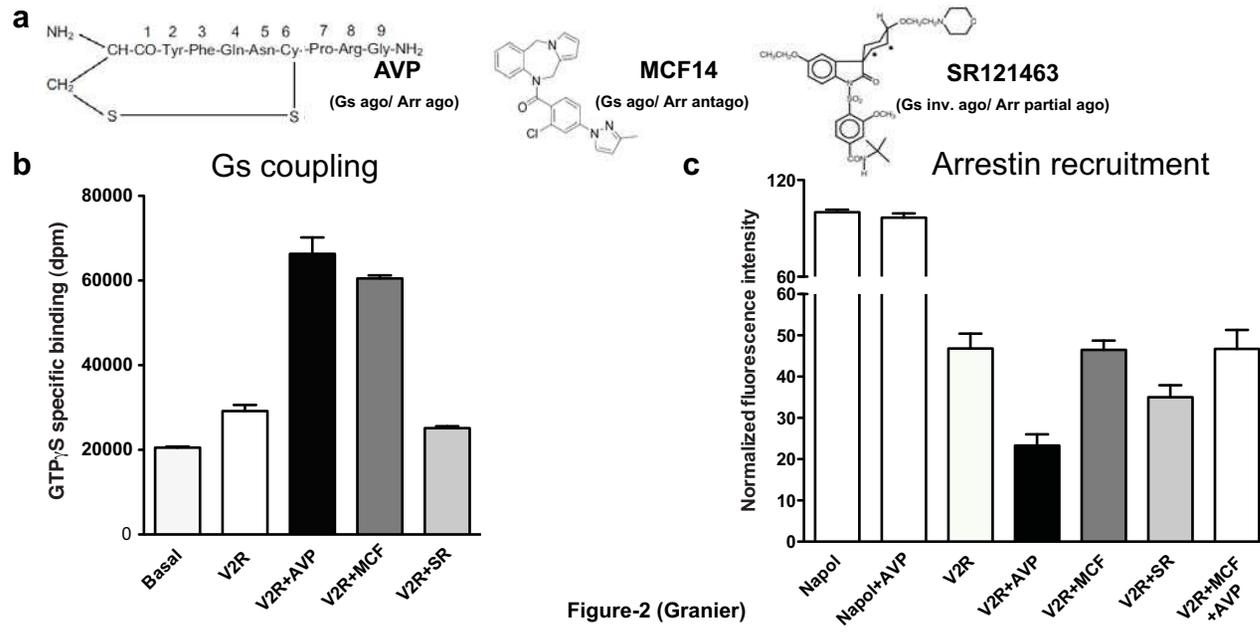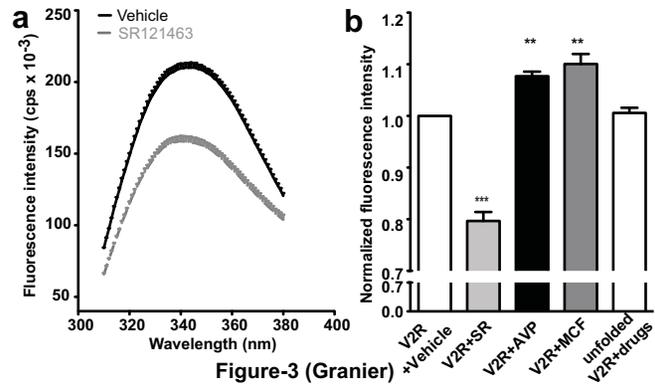
a Western Blot
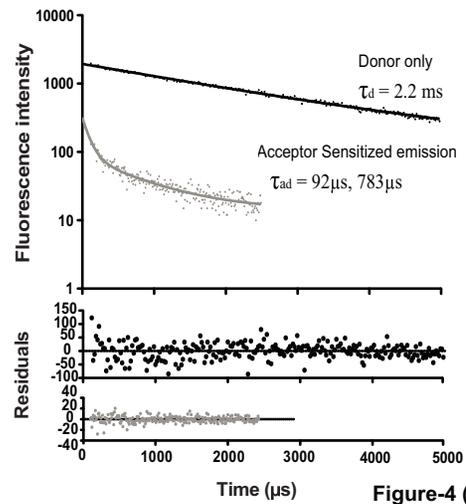
MW (kDa)

1 2 3

170
130
95 — V2R D.
55
43 — V2R M.
34
26

17

b

Absorbance at 280 nm (A.U.)

158 75 44 ← MW Standards (kDa)

MW Standards (kDa)
200
116
97
66
45

Napol-reconstituted V2R

Elution volume (ml)

Figure-1 (Granier)

c

Pop1 (32.6%)
7.5 nm

Pop2 (36%)
9.4 nm   9.3 nm

Pop3 (31.4%)
10.8 nm   10.4 nm

d

[³H]-AVP specific binding (cpm)

[³H]-AVP FREE (µM)

a

AVP (Gs ago/ Arr ago)

MCF14 (Gs ago/ Arr antago)

SR121463 (Gs inv. ago/ Arr partial ago)

b Gs coupling

c Arrestin recruitment

Figure-2 (Granier)

a

Fluorescence intensity (cps × 10⁻³)

— Vehicle
— SR121463

Wavelength (nm)

b

Normalized fluorescence intensity

V2R
+Vehicle

V2R+SR ***

V2R+AVP **

V2R+MCF **

unfolded
V2R+drugs

Figure-3 (Granier)

a

TM6
SENSOR

A267C TM6
icl3
Lumi-4 Tb
FlAsH

Donor only
τ_d = 2.2 ms

Acceptor Sensitized emission
τ_{ad} = 92μs, 783μs

Fluorescence intensity

Residuals

Time (μs)

b

TM7-H8
SENSOR

H8
S330C
icl3
Lumi-4 Tb
FlAsH

Donor only
τ_d = 2.2 ms

Acceptor Sensitized emission
τ_{ad} = 37μs, 333μs

Fluorescence intensity

Residuals

Time (μs)

Figure-4 (Granier)

Figure-5 (Granier)

a **Gs ligands efficacy**

b **Arrestin ligands efficacy**
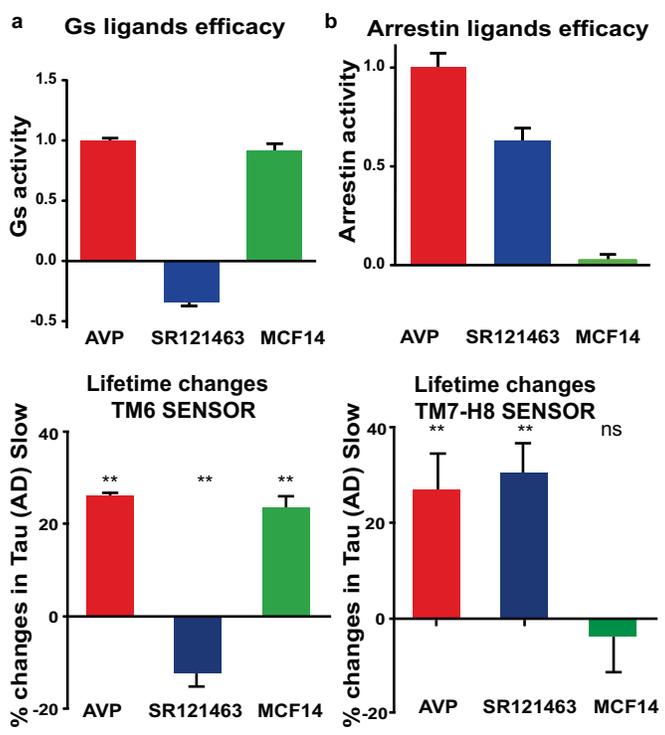

Lifetime changes TM6 SENSOR

Lifetime changes TM7-H8 SENSOR

Figure-6 (Granier)

Figure-7 (Granier)